

61016

Revised

Impact Melt Rock with Shocked/Melted Anorthosite Cap

11,745 grams



Figure 1: Close-up photo of a portion of the top surface of 61016,456 showing dimorphic nature of stone and numerous zap pits. Cube is 1 cm. NASA#S98-01215.

Introduction

Lunar sample 61016 is the largest sample returned by the Apollo missions. It is known as “Big Muley”; named after Bill Muehlberger, the leader of the Apollo 16 field geology team. It was found perched on the east rim of Plum Crater and its lunar orientation is roughly known from television photos and zap-pitted top surface (Sutton 1981).

The Apollo 16 site was chosen to be in the lunar highlands, so that material could be collected that was distinctly different from that which was sampled in the Maria (A11, A12, A15). The pre-mission mapping, and consensus opinion, was that the rocks from the Descartes site would be volcanic (Milton 1968; Hodges 1972). However, the majority of the material returned from Apollo 16 turned out to be breccia with high plagioclase content. Chemists initially thought that the melt rock samples from Apollo 16 were “high alumina

basalt”, but when these samples were found to have high siderophile content, the evidence for impact origin was clear (Hubbard et al. 1973; Dowty et al. 1973; James 1981). Post mission analysis has pointed to an origin of a large portion of the Apollo 16 material as basin ejecta from Nectaris (Turner 1977; Maurer et al. 1978; James 1981 and others).

61016 has a cosmic ray exposure age (1.8 m.y.) that links it to the ejecta from South Ray Crater (Eugster 1999). The top side of 61016 is rounded, with thin patina and numerous micrometeorite “zap” pits (figure 1). Solar-cosmic-ray-produced ^{21}Ne profiles verify the top surface was exposed to the Sun (Rao et al. 1993). Surface photography (television shot) of 61016 was matched in the laboratory by Sutton (1981) (figure 2). The sample was found partially buried – see soil line drawn on photos in Sutton (1981).



Figure 2: Photo of E1 side of 61016 with lighting similar to lunar lighting, thus providing knowledge of lunar orientation. Cube is 1 inch, showing approximate lunar orientation. NASA#S72-41841



Figure 3: Laboratory “mug shot” of E1 end of 61016, sitting on its flat bottom side. NASA photo# S72-41550. Scale same as for figure 2.

What was known about this rock in 1980 was discussed in great detail in the catalog by Ryder and Norman (1980). The rock has been highly shocked, as evidenced by most of the plagioclase being converted to maskelynite and/or plagioclase glass. Since 1980, the rock has been dated at about 3.97 ± 0.25 b.y. and used for determination of solar-cosmic-ray profile studies (see below). However, the petrology of the sample mostly remains undetermined.

Petrography

James (1981) has grouped 61016 with Apollo 16 samples termed “dimict” breccias, although the nature of 61016 is seemingly somewhat different (i.e. a piece of shocked anorthosite attached to a piece of troctolitic “melt rock”). Perhaps the best description of 61016 was provided by Stöffler et al. (1975), but this, the largest moon rock, seems to deserve further description in light of what is now known about lunar samples.

The majority of 61016 (figure 5) is apparently an impact “melt rock” with high Al_2O_3 (~25 wt %) and high KREEP content (figure 11). McGee et al. (1979) described the main lithology as “characterized by subangular to rounded clasts of partially to completely maskelynized plagioclase (up to 2 mm across) together with glassy and partially devirified lithic clast

contained in a subophitic matrix of tabular (0.1 to 0.2 mm) and lath-shaped (2 x 0.5 mm) maskelynite intergrown with subhedral to euhedral (0.1 mm) olivine crystals. A dark-brown glassy mesostasis fills interstices.” Because of its high modal olivine, Stöffler et al. (1975) termed this lithology as a “troctolitic matrix” and noted that all the plagioclase is diaplectic. (However, a high modal olivine content as reported by Stöffler is not consistent with the high Al_2O_3 content). This “melt rock” lithology is apparently unusual and is lacking pyroxene. The relict olivine is apparently mafic (~ Fe_{90}), while the relict plagioclase is calcic (~ An_{96}).

The shocked/melted anorthosite that sits as a “cap” on 61016 is described by Steele and Smith (1973), Smith and Steele (1974), Dixon and Papike (1975) and Drake (1974) and is one of the largest pieces of anorthosite returned. Pyroxene analyses from the anorthosite (figure 10) show that it is typical of ferroan anorthosite. The boundary between the melt rock lithology and this anorthosite is made of melted plagioclase (figure 30).

The bottom surface of 61016 is covered by glass (figure 4) where it was protected from meteorite bombardment. This glass coating may have originally covered the rest of the sample as though the rock was once a “bomb”.

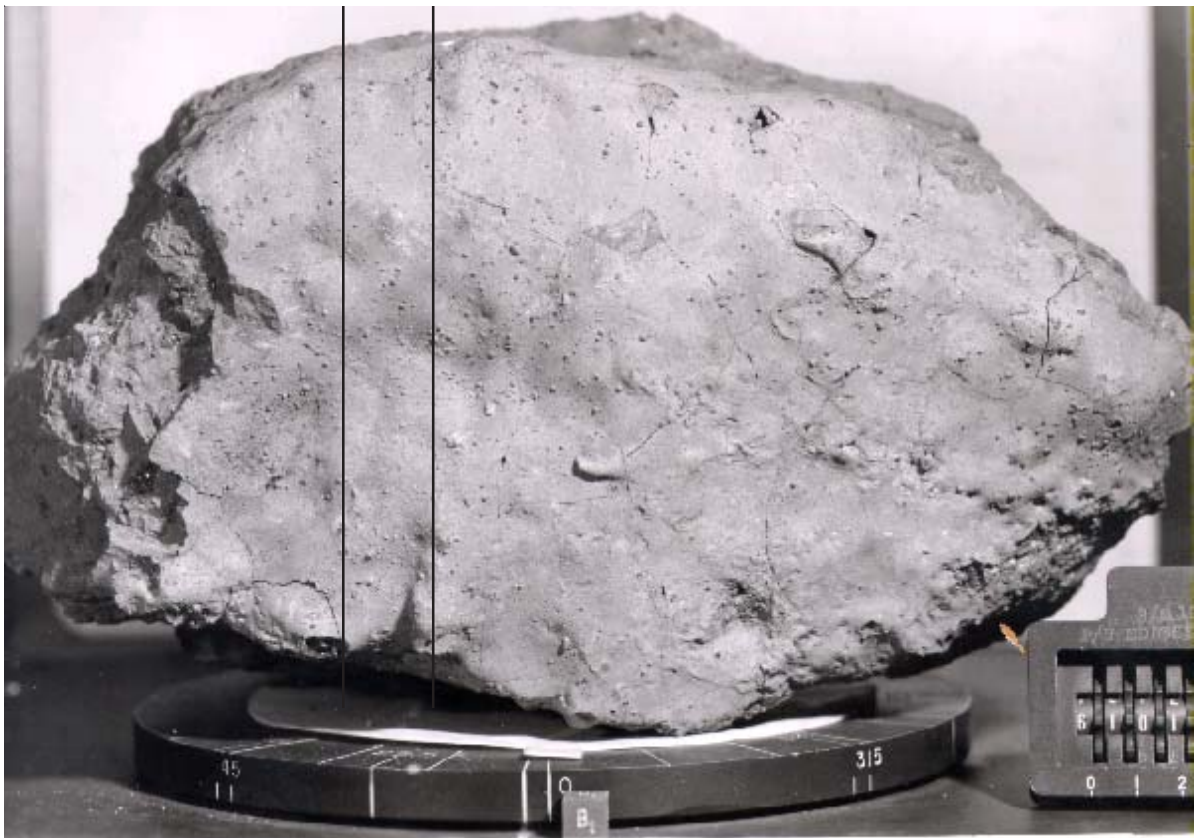


Figure 4: "Mug shot" of glass-coated bottom surface of 61016. Cube is 1 cm. NASA#S72-41556.

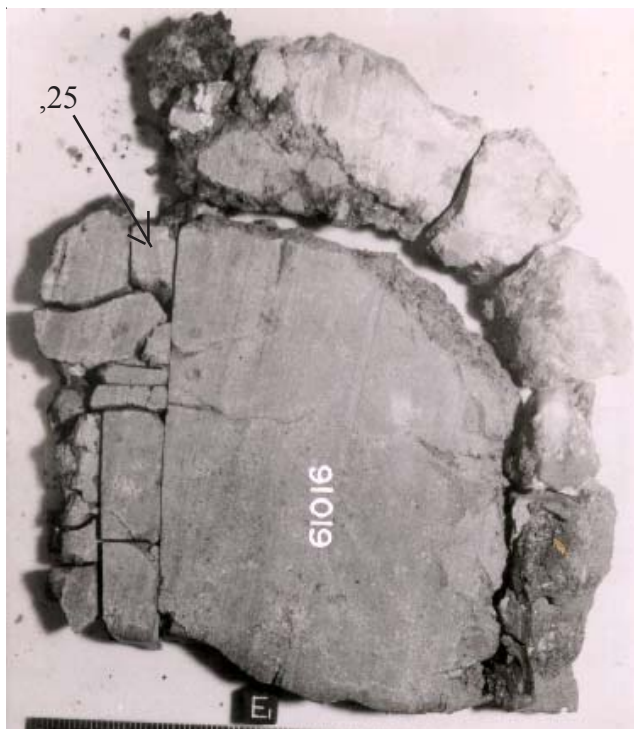


Figure 5: Photo of slab through middle of 61016 showing relation of anorthosite "cap" to the melt rock interior. Cube is 1 cm. NASA#S72-53505.

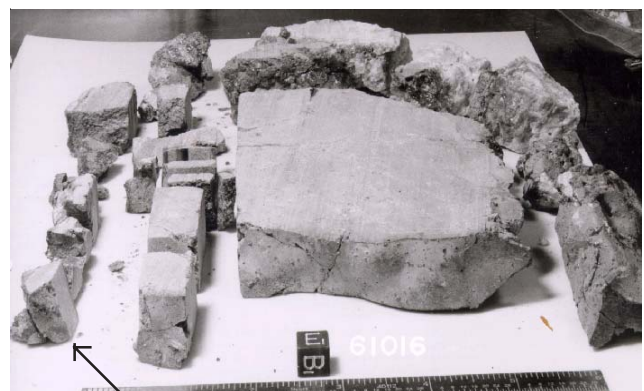


Figure 6: Exploded parts diagram for slab of 61016. NASA #S72-50676 (note glass coating on bottom)

See et al. (1986) and Stöffler et al. (1975) studied portions of the glass coating on 61016. There is reason to believe that 61016 was ejected from South Ray Crater.

Mineralogy

Olivine: Stöffler et al. (1975) found the olivine in the melt rock portion was Fo₈₂₋₉₃.



Figure 7: Thin section 61016,220 showing boundary of melt rock breccia and anorthosite cap (scale 20 mm).

Pyroxene: No pyroxene is reported from the melt rock portion, but pyroxene grains in the anorthosite portion are found to be Fe-rich (figure 10).

Plagioclase: Plagioclase in the melt rock portion is An₉₂₋₉₈. Hansen et al. (1979) have studied the trace elements in plagioclase in the anorthosite. Almost all plagioclase in this sample has been converted to maskelynite or plagioclase glass.

Metal: Misra and Taylor (1975) and Stöffler et al. (1975) found that metal grains in 61016 fell within the range of meteorite metal (Ni 4-8%; Co 0.3-0.5%).

Chemistry

On the basis of chemical composition, Hubbard et al. (1973) grouped the dark “melt rock” portion of 61016 with rocks they termed VHA basalts (VHA stands for very high alumina). The melt rock portion has high REE content (table 1, figure 11). Note that the meteoritic siderophiles in this portion are high. Ganapathy et al. (1974) place this melt rock in their meteorite Group 1. Stöffler et al. (1975) made chemical

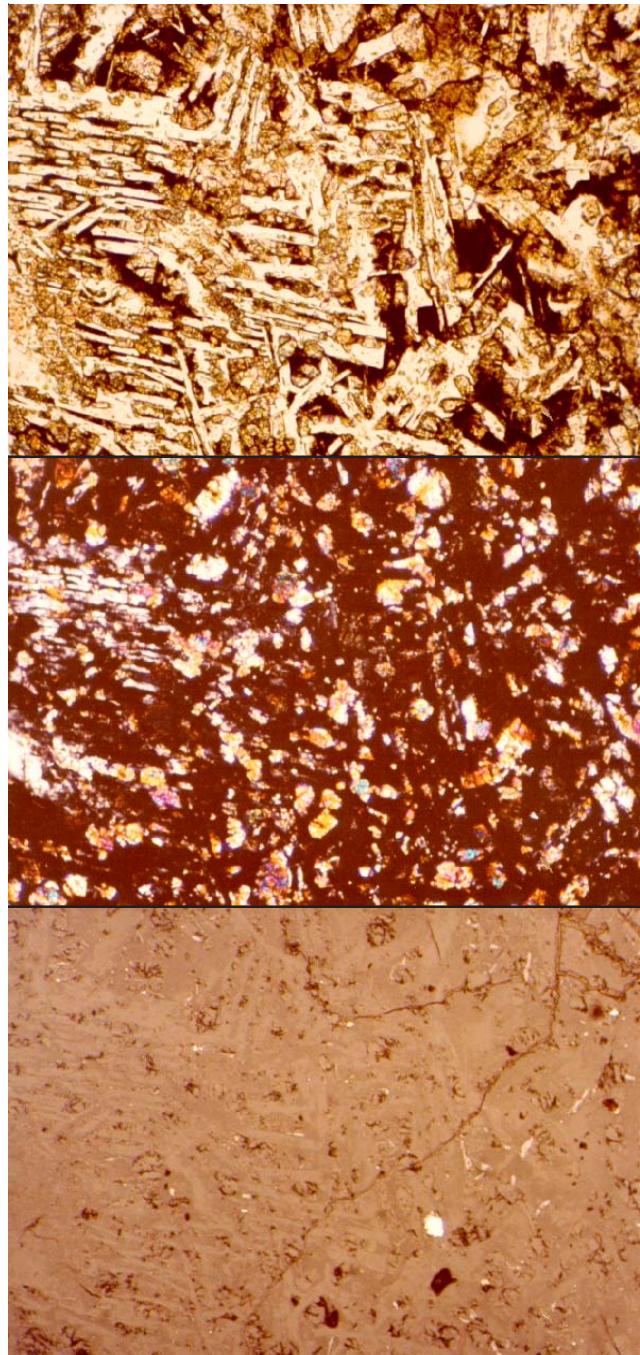


Figure 8: Three views (transmitted, X-nicol, and reflected) of same area (2.5 mm) within thin section 61016,220 showing that plagioclase is isotropic.

analyses of various portions of 61016 by broad beam electron microprobe technique and compared them with the experimental phase diagram of Walker et al. (1973). These analysis fall well off of the coetectic lines on the phase diagram (figure 13) showing that the areas analyzed are partially fused rock clasts and/or mixtures produced by secondary impact processes.

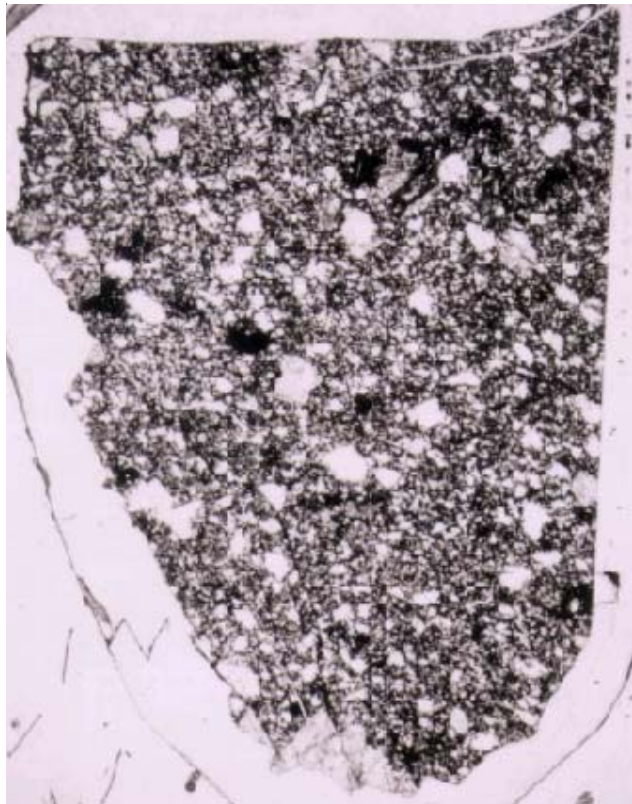


Figure 9: Photomicrograph of thin section from troctolitic "melt rock" portion of 61016,9 showing relict clastic texture (section is 20 mm across).

The anorthositic portion has been analyzed by Hubbard et al. (1974), Nava et al. (1974), Phillipotts et al. (1974) and others (table 2, figure 11). Meteoritic siderophiles in the anorthositic portion are low (Krahenbuhl et al. 1973) and it appears pristine (see figures 33, 34).

Stöffler et al. (1975), See et al. (1986) and Morris et al. (1986) determined the chemical composition of the glass coating (table 3, figure 12).

Radiogenic age dating

Stettler et al. (1973) reported an age of ~3.65 b.y., but this age is less than certain because they did not obtain a good Ar/Ar plateau (figure 14). Huneke et al. (1977) made several experiments to determine the age of the anorthosite (figure 15). Recently, Eugster et al. (1999) have dated the melt rock portion at 3.97 ± 0.25 b.y., seemingly consistent with the age of Nectaris (~3.95 b.y.) as determined by other rocks (see table).

Nyquist et al. (1973, 1979) determined Rb, Sr and $^{87}\text{Sr}/^{86}\text{Sr}$ for both main lithologies of 61016. The $^{87}\text{Sr}/^{86}\text{Sr}$ for the anorthosite was found to be very low (0.699).

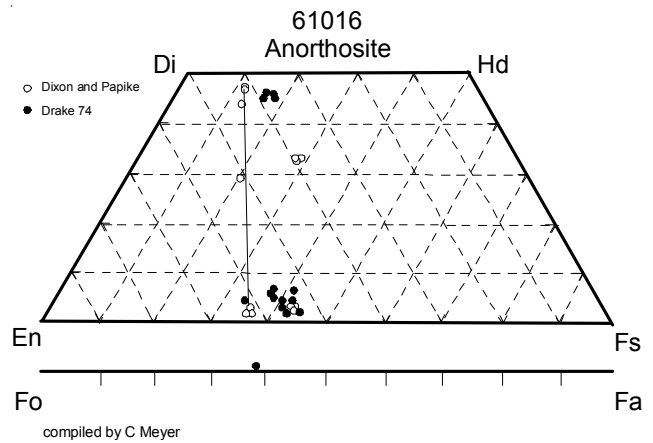


Figure 10: Pyroxene and olivine composition determined for the anorthositic portion of 61016,

Cosmogenic isotopes and exposure ages

Stettler et al. (1973) determined an exposure age of <7 m.y. by ^{38}Ar . Using sample ,287, Rao et al. (1979), Venkatesan et al. (1980), Nautiyal et al. (1981) and Rao et al. (1993) determined a cosmic ray exposure age of 1.7 ± 0.2 m.y. for an assumed erosion rate of 5 mm/m.y. Averaging the results from all techniques, Eugster (1999) determined an average cosmic ray exposure age of 1.84 ± 0.4 m.y. for 61016. This is consistent with ejecta from South Ray Crater.

Wrigley (1973) determined $^{26}\text{Al} = 104$ dpm/kg and $^{22}\text{Na} = 36$ dpm/kg on a 132 gram piece of anorthosite (,173). Eldridge et al. (1973) found $^{26}\text{Al} = 65$ dpm/kg and $^{22}\text{Na} = 30$ dpm/kg for 61016,120 (bottom piece of ,8, shielded by rock and soil). Bhandari et al. (1975, 1976) determined ^{26}Al depth profile.

Fleischer and Hart (1974) calculated cosmic-ray particle track ages of 20-40 m.y., whereas Bhattacharya and Bhandari (1975) obtained 1.7 m.y. using the same technique.

Rao et al. (1993) used the outer surface of 61016 to determine fine-scale, depth profiles for ^{21}Ne , ^{22}Ne and ^{38}Ar isotopes produced, in situ, from nuclear interactions of energetic solar flare protons (figure 17).

The density and size distribution of micrometeorite craters was studied by Mandeville et al. (1976) and Bhandari et al. (1975).

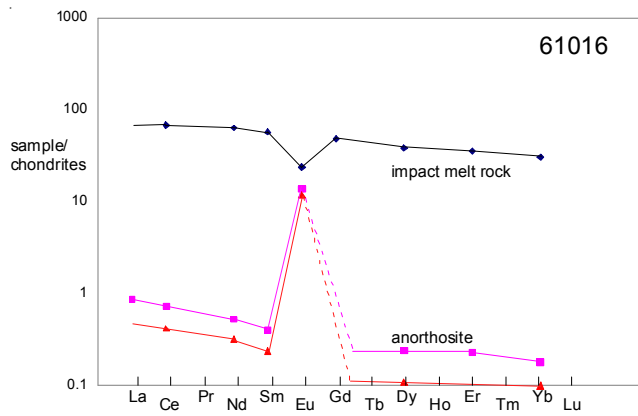


Figure 11: Rare-earth-element plot for 61016 interior melt rock and large anorthosite clast (i.d. data from Hubbard et al. 1974 and Philpotts et al. 1974, tables 1 and 2).

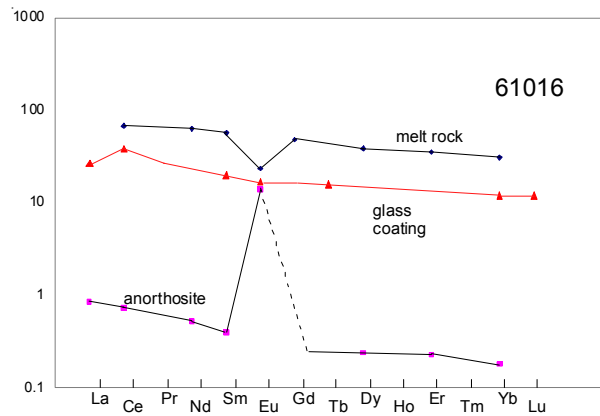


Figure 12: Rare-earth-element diagram for 61016 black glass coating (from Morris et al. 1986, table 3).

Other Studies

Reese and Thode 1974	S isotopes
Kerridge et al. 1975	S, C isotopes
DesMarais 1978	C isotopes
Allen et al. 1974	Pb isotopes
Tera et al. 1973	Pb isotopes
Nyquist et al. 1973	Sr isotopes
MacDougall et al 1973	tracks
Fleischer and Hart 1974	tracks
Bhattacharya, Bhandari 1975	tracks
Mandeville 1976	craters
Bhandari et al. 1975'	craters
Eldridge et al. 1973	²⁶ Al
Stephenson et al. 1977	magnetics
Housley et al. 1976	magnetics
Chung 1973	elastic wave velocity
Chung and Westphal 1973	electrical conductivity
Warren and Trice 1975	compressional modulus
Dolphus and Geake 1975	light polarization

Processing

In 1972 large thick slab (2 cm) was cut from the middle of 61016 (figures 4, 18-23). The east end piece (,8) and the slab have been entirely subdivided (figures 5,6). The large end piece (,7) remained unstudied until about 1990-94, when pieces of the anorthosite cap were removed (figures 23-25) for solar-cosmic-ray studies.

Subsamples ,385 and ,468 have been carefully sectioned to provide depth profiles of solar-flare-cosmic-ray radionuclide production (figures 16, 34).

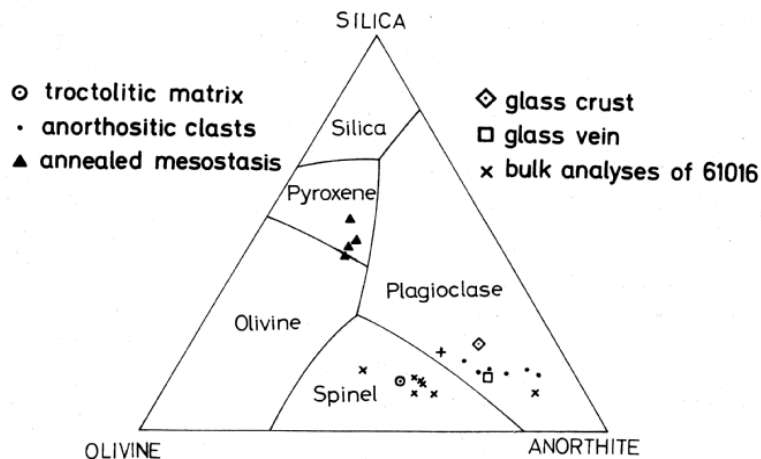


Figure 13: Broad beam electron microprobe analyses of regions within 61016 by Stoffler et al.

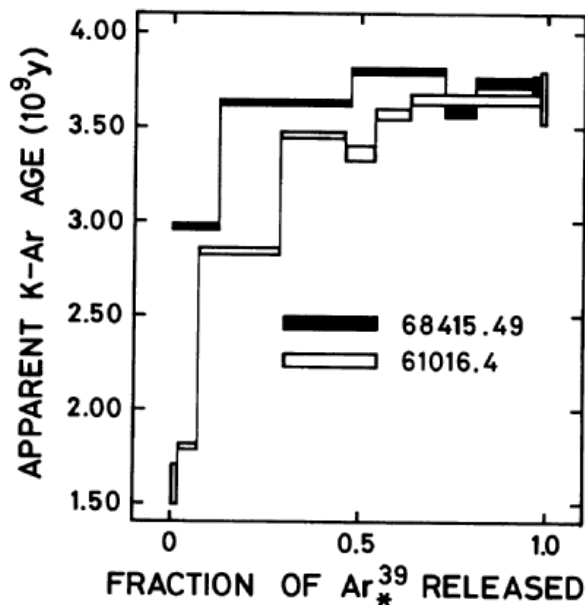


Figure 14: Ar release pattern for impact melt rock portion of 61016 (from Stettler et al. 1973).

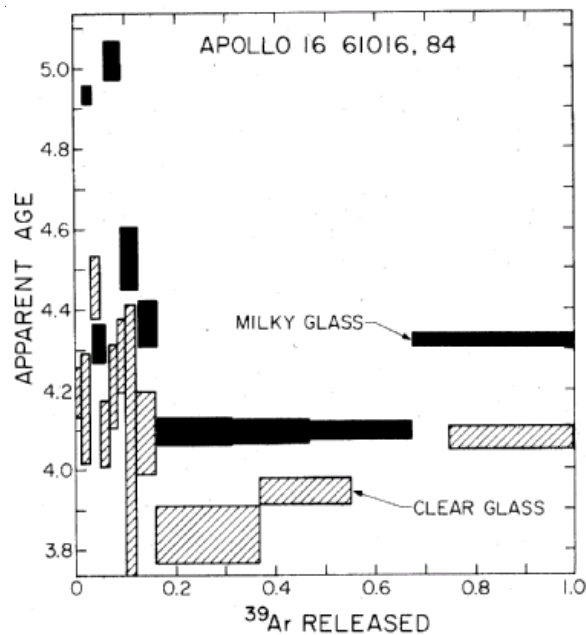


Figure 15: Ar release pattern for shocked - melted anorthositic portion of 61016 (from Huneke et al. 1977).

Summary of Age Data for 61016

	Ar39/40	U,Pu/ ¹³⁶ Xe
Stettler et al. 1973	~3.65 ± 0.04 b.y.	
Huneke et al. 1977	~4.1	
Eugster 1999		3.97 ± 0.25 b.y.

List of Photo #s for 61016.

S72-41841	lighting
S72-38970-38975	color mug shots
S72-41548-41563	B & W mug
S72-53505	slab
S72-50676	slab
S72-50691-50692	exploded parts
S72-51172-51171	,8 B & W
S75-33581	
S75-33567	
S75-33676	
S78-33099	
S78-33101	sawn surface ,7 color
S90-33268-33275	,385 prep
S93-45943-45944	
S94-39612-39630	,7
S98-01206-01216	,456
S99-11494-11507	,456 prep

Table 1a. Chemical composition of 61016 (melt rock).

reference	Impact melt matrix		Wiesmann 75		Wanke 74	Krahenbuhl 74	Rose 73	Laul 73	
	Ryder 80 average	Taylor 73	Hubbard 73						
SiO ₂ %	43.3	(e) 42.9			43.43	(e)	43.82		
TiO ₂	0.76	(e) 0.76	0.88	0.67	(d) 0.78	(e)	0.69	0.7	(a)
Al ₂ O ₃	25.1	(e) 23.9	24		24.56	(e)	25.06	25.6	(a)
FeO	5.1	(e) 5.31	5.4		5.16	(e)	4.97	5	(a)
MnO	0.05	(e)			0.05	(e)	0.05	0.052	(a)
MgO	10.7	(e) 12.5	11.5		10.26	(e)	10.48	10	(a)
CaO	14.3	(e) 13.3	13.7		14.42	(e)	14.31	14.4	(a)
Na ₂ O	0.33	(e) 0.29	0.29	0.31	0.36	(a)	0.36	0.346	(a)
K ₂ O	0.08	(e) 0.13	0.083	0.067	(d) 0.08	(a)	0.07	0.076	(a)
P ₂ O ₅	0.12	(e)			0.12	(a)	0.12		
S %									
sum									
Sc ppm	6.6	(e) 3.5	(c)		6.6	(a)	6.6	7.4	(a)
V		21	(c)				15	20	(a)
Cr		250	(c) 697	433	(d) 600	(e)	752	643	(a)
Co	36	(e) 35	(c)		36.7	(a)	34	37	(a)
Ni	443	(e) 480	(c)		510	(a)	515	345	(f) 350
Cu	4.4	(e) 2.3	(c)		6.4	(a)	0.84	0.74	(f) 3.3
Zn									
Ga					3.48	(a)			2.4
Ge ppb					850	(a)	620	353	(f)
As					270	(a)			
Se							181	112	(f)
Rb	2	(e) 1.8	(c) 2.04	1.63	(d) 2.84	(a)	2	1.3	(f) 1.8
Sr	160	(e)	166	170	(d) 130	(a)			110
Y		60	(c)		44	(a)			34
Zr		295	(c) 243		(d) 209	(a)			150
Nb		20.5	(c)		13	(a)			10
Mo									
Ru									
Rh									
Pd ppb					25	(a)			
Ag ppb							21.4	1.7	(f)
Cd ppb							29.5	9.6	(f)
In ppb									
Sn ppb									
Sb ppb							3.13	1.74	(f)
Te ppb							4.8	5.7	(f)
Cs ppm					0.12	(a)	0.084	0.056	(f)
Ba		240	(c) 172	137	(d) 160	(a)		105	
La	15.3	(e) 19.2	(c)	13	(d) 16.7	(a)			130
Ce		52	(c) 41.8	32.7	(d) 46	(a)			14.9
Pr		6.71	(c)		5.8	(a)			39
Nd		25.9	(c) 29.2	21.2	(d)				28
Sm		7	(c) 8.5	5.88	(d) 6.9	(a)			7
Eu		1.23	(c) 1.38	1.28	(d) 1.38	(a)			1.42
Gd		9.1	(c) 9.67	7.46	(d) 9.5	(a)			
Tb		1.28	(c)		1.5	(a)			1.3
Dy		8.5	(c) 9.4	7.5	(d) 9.7	(a)			8.5
Ho		1.83	(c)		2	(a)			
Er		5.4	(c) 5.68	4.38	(d) 4.8	(a)			
Tm		0.84	(c)						
Yb		5.1	(c) 4.97	3.87	(d) 4.4	(a)		2.8	
Lu	0.65	(e) 0.79	(c)		(d) 0.61	(a)			4.3
Hf		4.2	(c) 5.99		(d) 4.9	(a)			0.6
Ta					1.02	(a)			5.2
W ppb					0.25	(a)			0.73
Re ppb					14	(a)	1.28	0.841	(f)
Os ppb									
Ir ppb	13	(e)			15	(a)	11.5	6.67	(f)
Pt ppb									
Au ppb	12	(e)			13	(a)	9.55	5.6	(f)
Th ppm			2.38		(d) 1.6	(a)			14
U ppm			0.497	0.394	(d) 0.46	(a)			2.1
technique:									0.47

technique: (a) INAA, (b) el. probe, (c) SSMS, (d) IDMS, (e) average value, (f) RNAA

Table 1b. Chemical composition of 61016 (melt rock).

reference weight	Nakamura 73,148	Garg 76		Wasson 75	Brunfelt 73	Eldridge 73,120	Juan 74,146	
SiO2 %	43.2						44	(c)
TiO2	0.6				1.1		0.66	(c)
Al2O3	24.8				26.26		24.9	(c)
FeO	5.11	4.82	(a)		4.63		4.5	(c)
MnO	0.057				0.057		0.04	(c)
MgO	9.18				9.12		11	(c)
CaO	15.14				15.25		14.8	(c)
Na2O	0.37				0.34		0.4	(c)
K2O	0.09				0.078	0.067	0.07	(c)
P2O5	0.101							(b)
S %								
sum								
Sc ppm		6.3	(a)		5.9	(a)		
V					40	(a)		
Cr		560	(a)		650	(a)	600	(c)
Co		37	(a)		33	(a)	51	(c)
Ni				569	(a) 540	(a)	268	(c)
Cu					6.6	(a)	2	(c)
Zn				0.52	(a) 3.4	(a)		(c)
Ga				3.69	(a) 2.5	(a)		
Ge ppb				641	(a)			
As								
Se								
Rb					3.2	(a)	2.1	(c)
Sr							180	(c)
Y								
Zr		224	196	(a)				
Nb								
Mo								
Ru								
Rh								
Pd ppb								
Ag ppb								
Cd ppb				8	(a)			
In ppb				4	(a) 10	(a)		
Sn ppb								
Sb ppb								
Te ppb								
Cs ppm						0.17	(a)	
Ba	152	(d)				125	(a)	
La	13	(d)				15.6	(a)	
Ce	34.12	(d) 34.7	(a)			40	(a)	
Pr								
Nd	21.91	(d)						
Sm	6.181	(d)				6.8	(a)	
Eu	1.346	(d) 1.17	(a)			1.53	(a)	
Gd	7.245	(d)						
Tb		1.1	(a)			1.02	(a)	
Dy	7.64	(d)				7.3	(a)	
Ho						1.6	(a)	
Er	4.42	(d)				4.4	(a)	
Tm								
Yb	3.96	(d)				3.9	(a)	
Lu	0.557	(d) 0.87	(a)			0.72	(a)	
Hf		4.72	4.42	(a)		4.5	(a)	
Ta						0.45	(a)	
W ppb								
Re ppb								
Os ppb								
Ir ppb				15	(a)			
Pt ppb								
Au ppb				9.7	(a)			
Th ppm		1.4	(a)			1.7	(a) 1.84	(b)
U ppm						0.73	(a) 0.38	(b)

technique: (a) INAA, (b) radiation counting, (c) AAS and coloremtric

Table 2a. Chemical composition of 61016 (anorthosite?).

reference weight	Wiesmann 75						Ryder 80 average	Nava 74 ,184	Philpotts 74 ,184	Krahenbuhl ,156	Fruchter 74 ,180	
	LSPET 73 ,3	Hubbard 74 ,3	Hubbard 74 ,79	grey plag. ,84								
SiO2 %	44.15	(a)					45	45				
TiO2	0.2	(a)	0.18	0.02	0.02	0.017	(b) 0.02	0.02				
Al2O3	33.19	(a)					34.6	34.85			34.39	(c)
FeO	1.4	(a)					0.3				0.26	(c)
MnO	0.02	(a)										
MgO	2.51	(a)		0.16	0.25	0.16	(b) 0.2					
CaO	18.3	(a)					19.6	19.58				
Na2O	0.34	(a)	0.34	0.43	0.32	0.32	0.4	0.41			0.41	(c)
K2O	0.02	(a)	0.022	0.088	0.005	0.0048	(b) 0.01	0.005	0.0054	(b)		
P2O5	0.05	(a)					0.05	0.047				
S %	0.01	(a)										
sum												
Sc ppm							0.5				0.5	(c)
V												
Cr	200	(a)	190		375	<40	(b)				21	(c)
Co											0.5	(c)
Ni	39	(a)					~ 1			<1	(d)	
Cu												
Zn										1.45	(d)	
Ga												
Ge ppb										13	(d)	
As												
Se										0.4	(d)	
Rb	0.7	(a)	0.446	0.038	0.017	0.04	(b) 0.1		0.03	(b) 0.018	(d)	
Sr	179	(a)	177.9	180.4	179	182	(b) 180		149	(b)		
Y	11	(a)										
Zr	48	(a)	51.2	3	2		(b)					
Nb	2.4	(a)										
Mo												
Ru												
Rh												
Pd ppb												
Ag ppb										0.29	(d)	
Cd ppb										190	(d)	
In ppb												
Sn ppb												
Sb ppb										0.15	(d)	
Te ppb										<0.4	(d)	
Cs ppm										0.0012	(d)	
Ba			40.7	6.97	7.05	7.11	(b)		6.01	(b)		
La			3.47		0.143	0.204	(b) 0.1					
Ce			8.61		0.37	0.44	(b)		0.253	(b)	0.3	(c)
Pr												
Nd			5.6	0.2	0.205	0.239	(b)		0.145	(b)		
Sm			1.56	0.045	0.058	0.058	(b)		0.036	(b)	0.1	(c)
Eu			0.926	0.805	0.77	0.814	(b)		0.671	(b)		
Gd			1.84	0.045	0.054		(b)					
Tb											0.9	(c)
Dy			1.91	0.025	0.065	0.059	(b)		0.027	(b)		
Ho												
Er			1.16	0.067	0.04	0.037	(b)		0.014	(b)		
Tm												
Yb			1.01	0.02	0.045	0.03	(b)		0.017	(b)		
Lu			0.149	0.005	0.024		(b) 0.01					
Hf			1.06									
Ta												
W ppb												
Re ppb												
Os ppb												
Ir ppb												
Pt ppb												
Au ppb												
Th ppm	1.7	(a)	0.486									
U ppm			0.101	0.002	0.002		(b)			0.0009	(d)	
technique	(a) XRF, (b) IDMS, (c) INAA, (d) RNAA											

Table 2b. Chemical composition of 61016 (anorthosite?).

reference	,173	Baedecker 74		
weight	Wrigley 73	Wasson 75	Hughes 73	
	132 gr	,161		
SiO2 %				
TiO2				
Al2O3				
FeO				
MnO				
MgO				
CaO				
Na2O				
K2O	0.0084	(a)		
P2O5				
S %				
sum				
Sc ppm				
V				
Cr				
Co				
Ni		3.1	(b)	
Cu				
Zn		1.7	(b)	
Ga		3.46	(b)	
Ge ppb		23	(b)	
As				
Se				
Rb				
Sr				
Y				
Zr				
Nb				
Mo				
Ru				
Rh				
Pd ppb				
Ag ppb			0.6	(b)
Cd ppb		170	(b)	
In ppb		250	(b)	
Sn ppb				
Sb ppb				
Te ppb				
Cs ppm				
Ba				
La				
Ce				
Pr				
Nd				
Sm				
Eu				
Gd				
Tb				
Dy				
Ho				
Er				
Tm				
Yb				
Lu				
Hf				
Ta				
W ppb				
Re ppb			0.018	
Os ppb			0.72	
Ir ppb		0.2	(b)	0.82
Pt ppb				
Au ppb		0.94	(b)	0.024
Th ppm	0.11			
U ppm	0.05	(a)		

technique (a) radiation counting, (b) INAA

Table 3. Chemical composition of 61016 black glass.

reference weight	glass		black	
	Stoffler 75	Morris 86 See 86	Hubbard 74 glass	
SiO ₂ %	44.48	(a) 44.12	(b)	
TiO ₂	0.17	(a) 0.19	(b) 0.43	(d)
Al ₂ O ₃	29.83	(a) 31.74	(b)	
FeO	3.65	(a) 3.1	(b)	
MnO				
MgO	4.87	(a) 3.22	(b)	
CaO	15.64	(a) 17.51	(b)	
Na ₂ O	0.66	(a) 0.34	(b) 0.42	
K ₂ O	0.08	(a) 0.07	(b) 0.1	(d)
P ₂ O ₅	0.08	(a)		
S %				
sum				
Sc ppm		3.75	(c)	
V				
Cr		480	(c) 861	(d)
Co		24	(c)	
Ni		280	(c)	
Cu				
Zn				
Ga				
Ge ppb				
As				
Se				
Rb			1.877	(d)
Sr			145	(d)
Y				
Zr			190	(d)
Nb				
Mo				
Ru				
Rh				
Pd ppb				
Ag ppb				
Cd ppb				
In ppb				
Sn ppb				
Sb ppb				
Te ppb				
Cs ppm				
Ba			132	(d)
La		6.3	(c) 13.6	(d)
Ce		23.5	(c) 29.8	(d)
Pr				
Nd			10.9	(d)
Sm		3	(c) 3.06	(d)
Eu		0.97	(c) 0.526	(d)
Gd			3.61	(d)
Tb		0.59	(c)	
Dy			7.9	(d)
Ho				
Er			5.1	(d)
Tm				
Yb		2	(c) 4.25	(d)
Lu		0.29	(c) 0.619	(d)
Hf		2.25	(c) 3.8	(d)
Ta				
W ppb				
Re ppb				
Os ppb				
Ir ppb				
Pt ppb				
Au ppb				
Th ppm		0.59	(c) 2.07	(d)
U ppm		0.09	(c) 0.6	(d)

technique (a) el. Probe, (b) (c) INAA, (d) IDMS

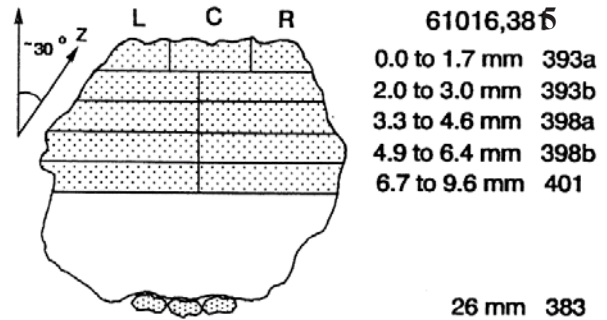


Figure 16: Near surface sample of 61016,385 used for solar cosmic ray profiles by Rao et al. 1993.

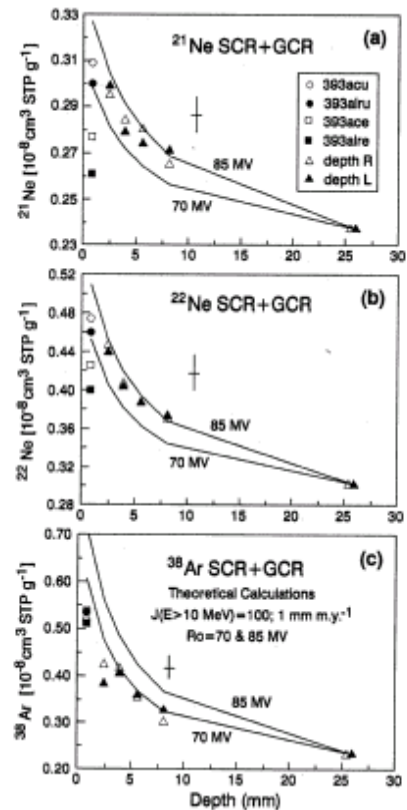


Figure 17: Solar cosmic ray profiles in surface samples of 61016 (from Rao et al. 1993).

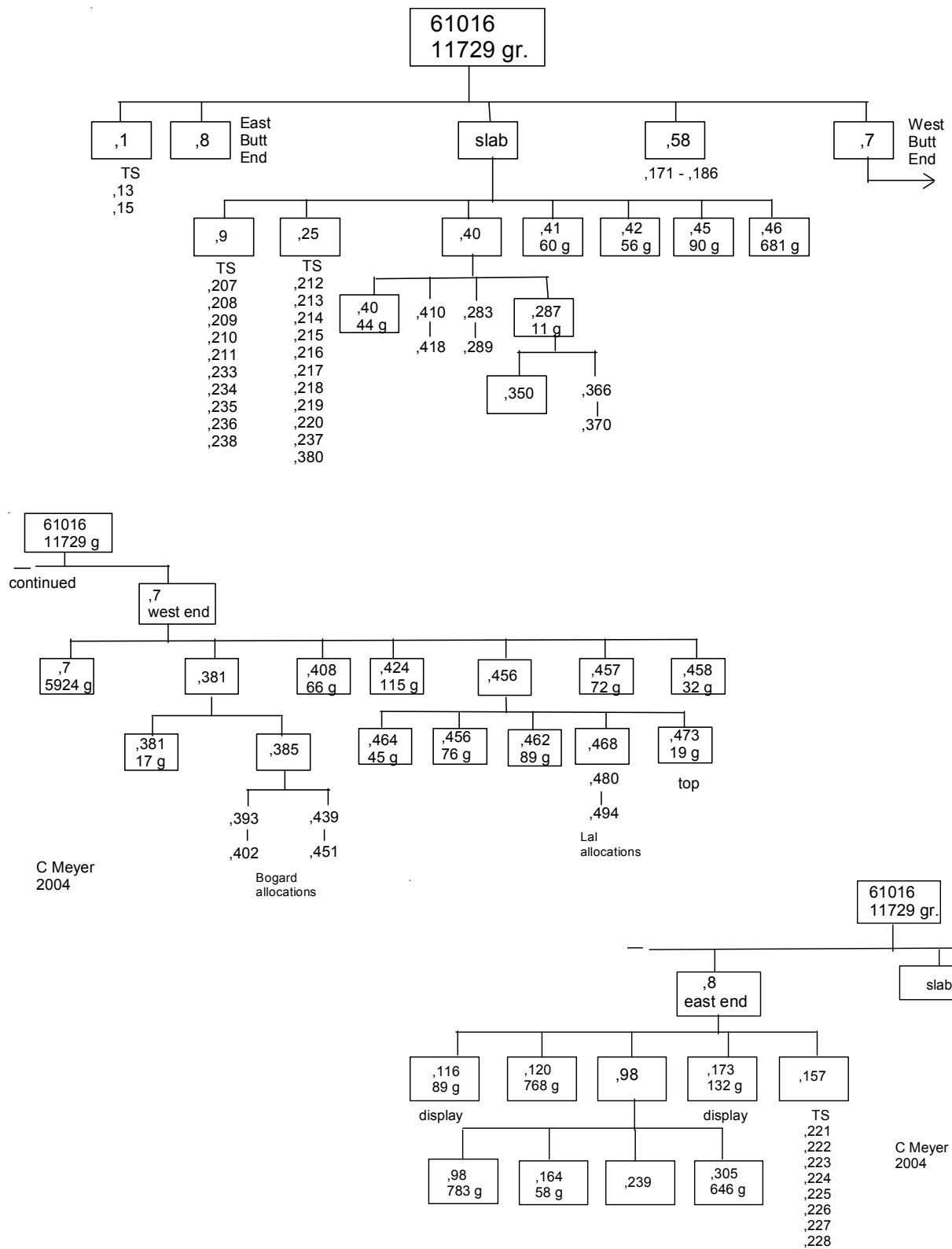


Figure 18: Generalized flow diagram for 61016 showing subdivisions (see pictures for details). Caution: not all samples shown.

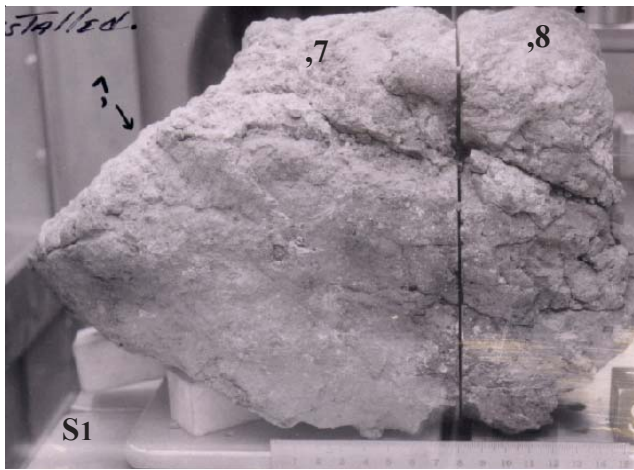


Figure 19: First saw cut 61016 (from data pack).

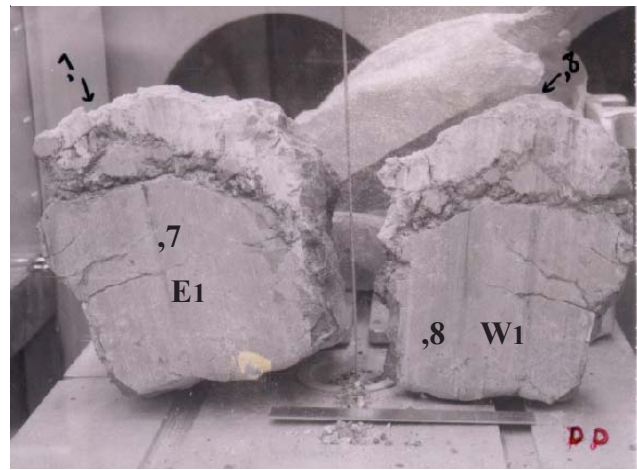


Figure 21: Sawn surfaces of 61016 after first saw cut showing anorthosite "cap" on dense, dark gray, "melt rock" interior (from data pack). Figure shows E1 face of large butt end, 7 (before slab is cut) and W1 face of butt end, 8 (see figure).

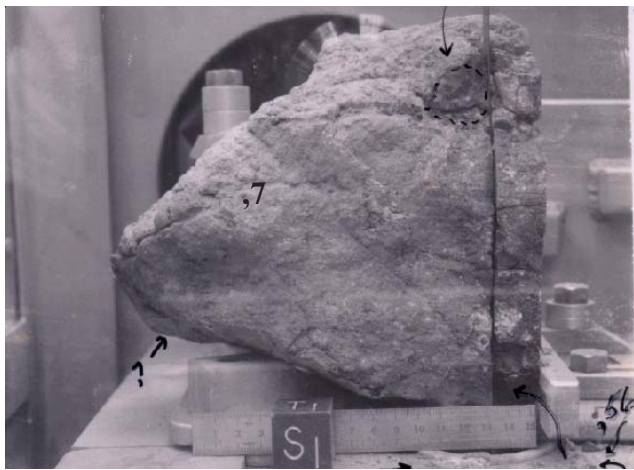


Figure 20: Position of second saw cut of 61016 in 1972 producing 2 cm thick slab (see flow diagram).

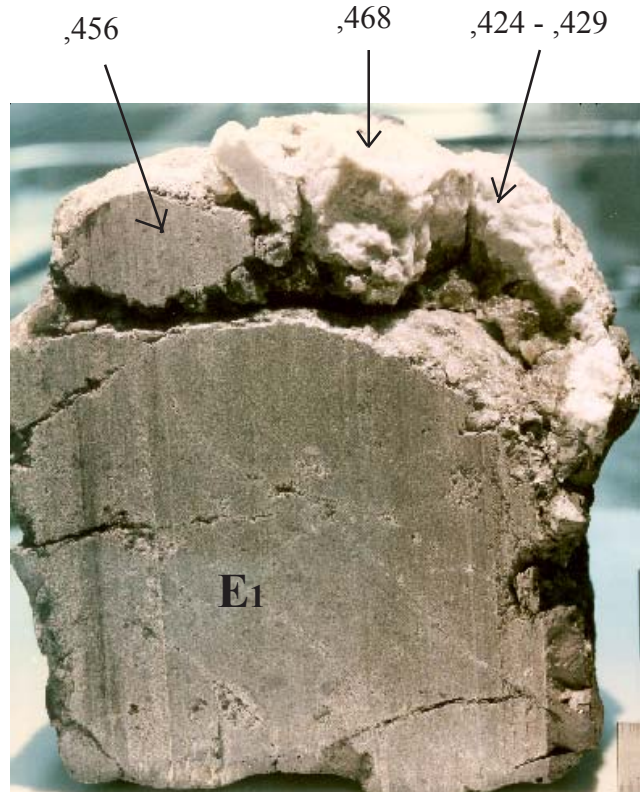


Figure 23: Sawn surface of 61016,7 (west end piece) showing E1 face and position of subsamples on top. Subsamples ,381, ,385 and ,408 (already removed) were in front of ,424-429. NASA S94-39613. One inch cube seen in bottom corner. Compare with figure 22.

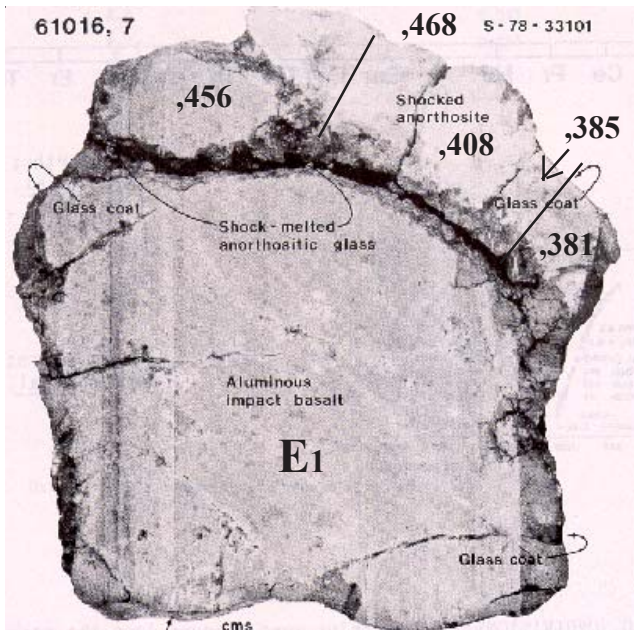


Figure 22: Photo after 2nd saw cut of 61016,7 (from Ryder and Norman 1980).

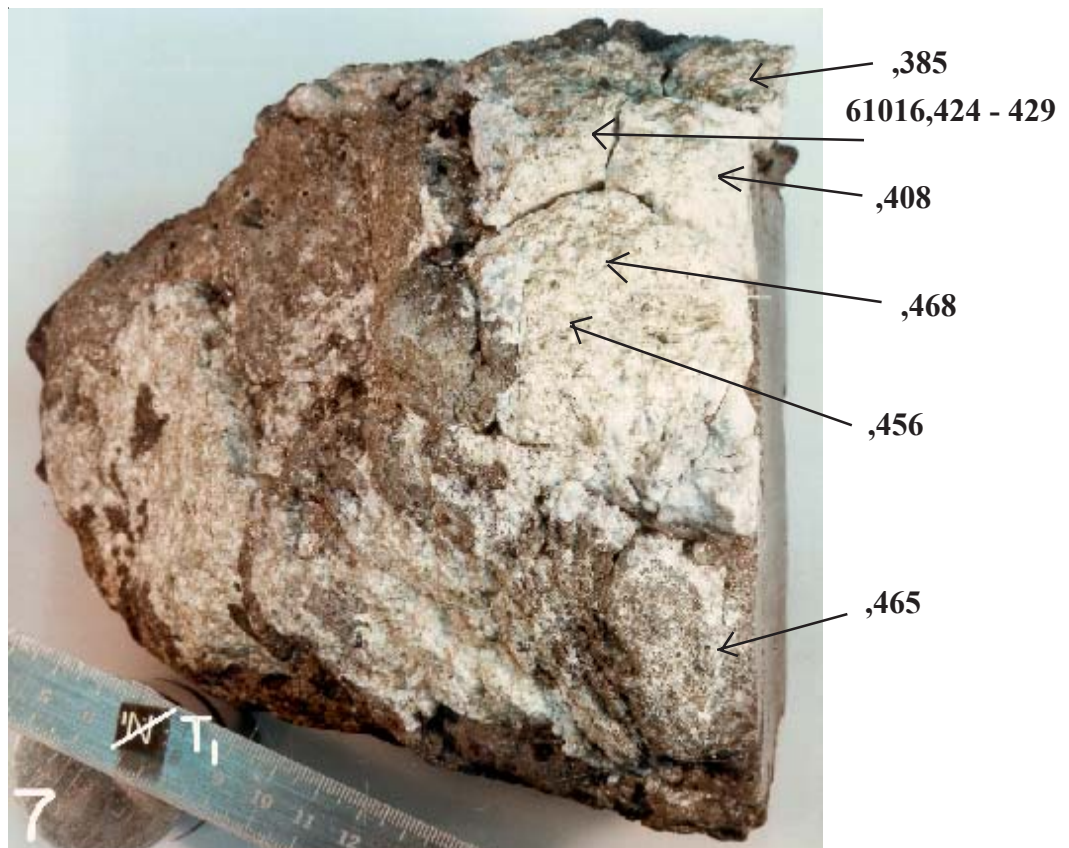


Figure 24: Photo of top surface of 61016,7, showing thin brown patina on anorthosite and zap pits all over. NASA# S78-33099. Cube is 1 cm. Compare with figures 1 and 23.

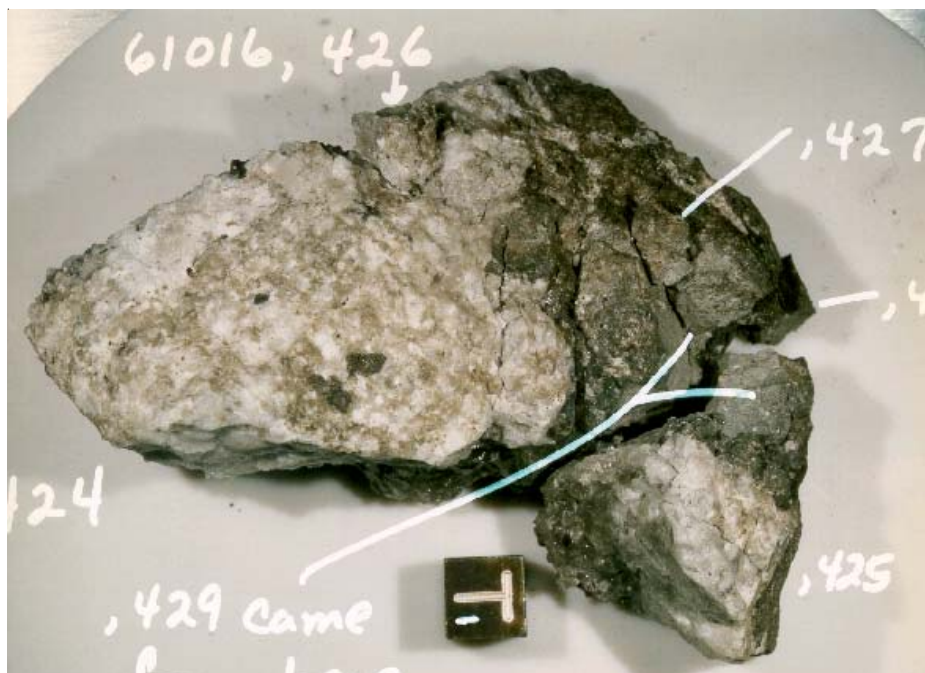


Figure 25: Top surface of 61016 facing the sun. Note the light brown patina on pure white anorthosite. NASA# S94-39620. Cube is 1 cm. (see figure 24).

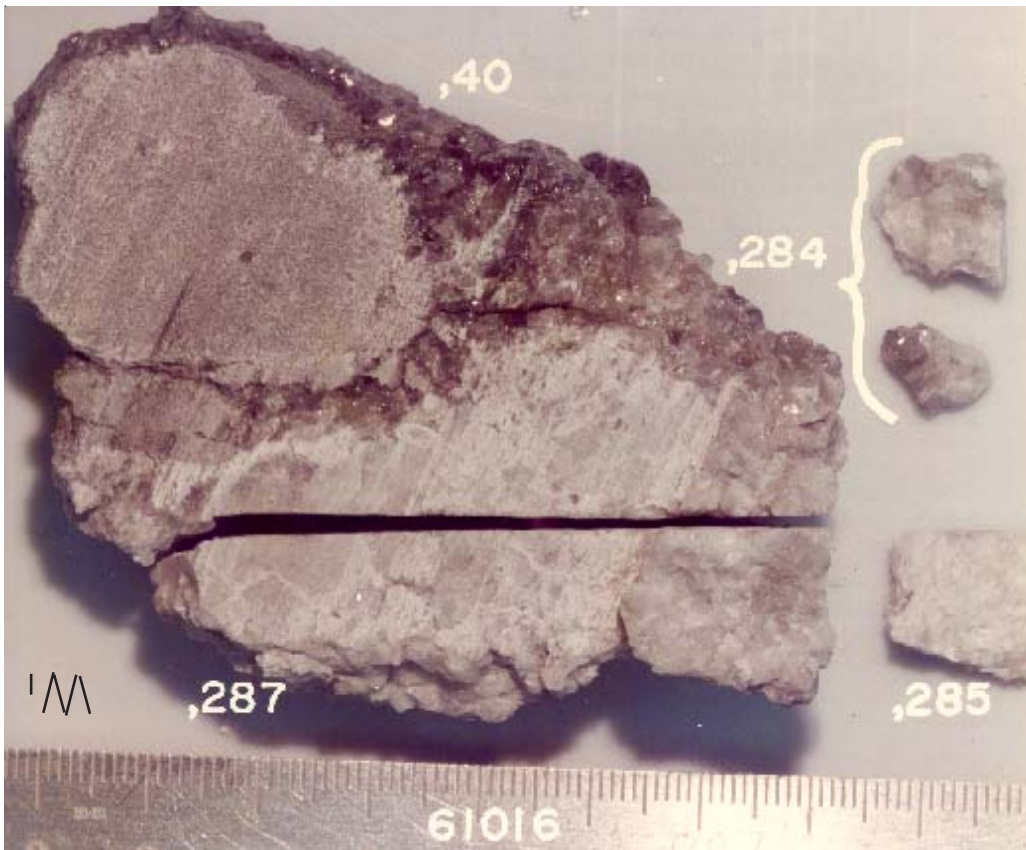


Figure 26: Photo of top portion of slab from 61016 (with T1 surface facing the ruler). NASA S74-33208. Scale in cm. Compare with figure 5 (top piece).



Figure 27: 61016,40 after sawing off the top (287). Small cube is 1 cm. NASA S74-33206. Streaks are from saw blade.



Figure 28: Top portion of 61016,8 showing an-orthosite cap with thin brown patina. Compare with figure 3. NASA #S75-33567. Cube is 1 cm.

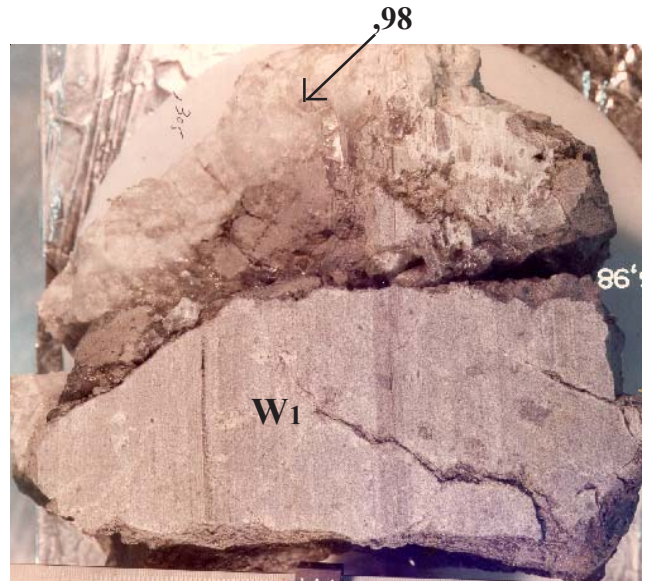


Figure 29: Top portion of 61016,8 (the east end piece) showing the W1 face (see figure 28). NASA #S75-33676. Cube is 1 cm



Figure 30: Plagioclase glass boundary on bottom surface of 61016,98. Cube is 1 cm. NASA S75-33581.

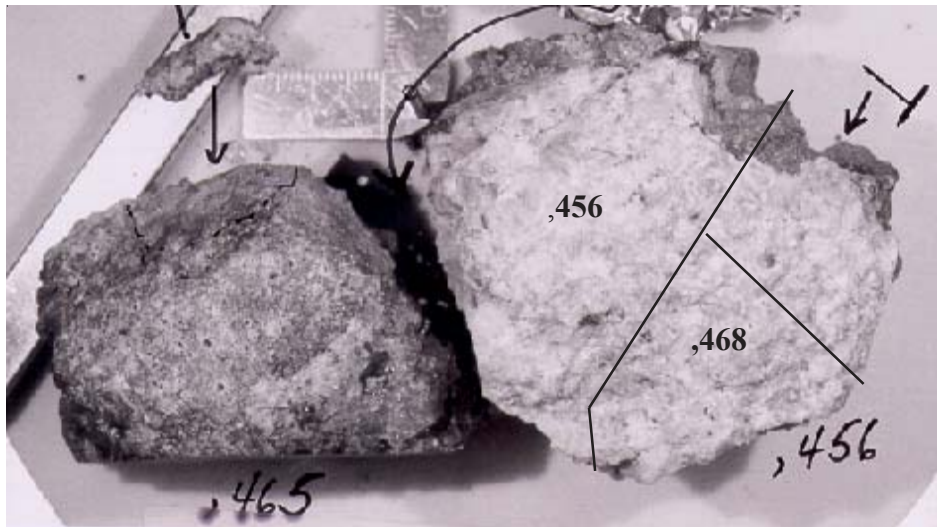


Figure 31: Photo of top of 61016,456 (from top of butt end,7). Compare with figures 1 and 24. Scale is in cm. Location of cuts is approximate. Photo from data pack.



Figure 32: Saw cut through 61016,456, producing ,468. Cube is 1 inch (cm scale in background). Photo from data pack.

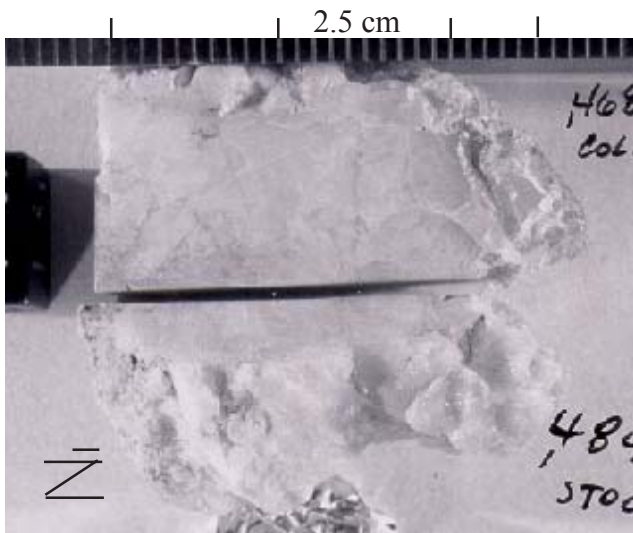


Figure 33: Photo of 61016,468 after sawing ,484.

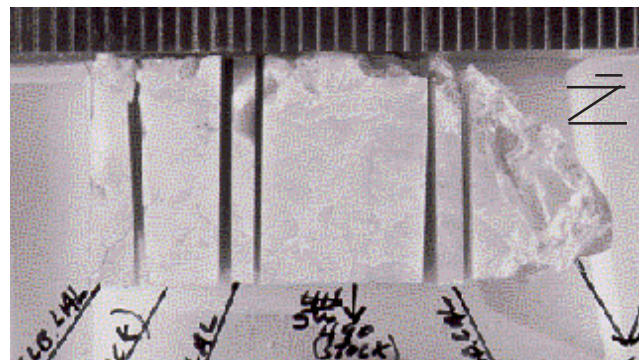


Figure 34: Saw cuts of ,468. Scale in mm. Photo from data pack.

References for 61016

- Allen R.O., Jovanovic S. and Reed G.W. (1974) A study of 204Pb partition in lunar samples using terrestrial and meteoritic analogs. *Proc. 5th Lunar Sci. Conf.* 1617-1623.
- Bhandari N., Bhattacharya S.K. and Padia J.T. (1975) The surface radioactivity of lunar rocks: Implications to solar activity in the past. *Proc. 6th Lunar Sci. Conf.* 1913-1925.
- Bhandari N., Bhattacharya S.K. and Padia J.T. (1976a) Solar proton fluxes during the last million years. *Proc. 7th Lunar Sci. Conf.* 513-523.
- Bhandari N., Bhattacharya S.K. and Padia J.T. (1976b) Solar flare records in lunar rocks (abs). *Lunar Sci. VII*, 49-51. Lunar Planetary Institute, Houston.
- Bhattacharya S.K., Goswami J.N., Lal D., Patel P.P. and Rao M.N. (1975) Lunar regolith and gas-rich meteorites: Characterization based on particle tracks and grain-size distributions. *Proc. 6th Lunar Sci. Conf.* 3509-3526.
- Dixon J.R. and Papike J.J. (1975) Petrology of anorthosites from the Descartes region of the moon: Apollo 16. *Proc. 6th Lunar Sci. Conf.* 263-291.
- Des Marais D.J. (1978a) Carbon, nitrogen and sulfur in Apollo 15, 16 and 17 rocks. *Proc. 9th Lunar Planet. Sci. Conf.* 2451-2467.
- Dowty E., Prinz M. and Keil K. (1974b) Ferroan anorthosite: a widespread and distinctive lunar rock type. *Earth Planet. Sci. Lett.* **24**, 15-25.
- Dollfus A. and Geake J.E. (1975) Polarimetric properties of the lunar surface and its interpretation: Part 7 – Other solar system objects. *Proc. 6th Lunar Sci. Conf.* 2749-2768.
- Drake M.J. (1975) Lunar anorthosite paradox. *Proc. 6th Lunar Sci. Conf.* 293-299.
- Eugster O. (1999) Chronology of dimict breccias and the age of South Ray crater at the Apollo 16 site. *Meteor. & Planet. Sci.* **34**, 385-391.
- Eldridge J.S., O'Kelley G.D. and Northcutt K.J. (1973) Radionuclide concentrations in Apollo 16 lunar samples determined by nondestructive gamma-ray spectrometry. *Proc. 4th Lunar Sci. Conf.* 2115-2122.
- Fleischer R.L. and Hart H.R. (1974b) Particle track record of Apollo 16 rocks from Plum crater. *J. Geophys. Res.* **79**, 766-769.
- Ganapathy R., Morgan J.W., Higuchi H., Anders E. and Anderson A.T. (1974) Meteoritic and volatile elements in Apollo 16 rocks and in separated phases from 14306. *Proc. 5th Lunar Sci. Conf.* 1659-1683.
- Hansen E.C., Steele I.M. and Smith J.V. (1979a) Lunar highland rocks: Element partitioning among minerals 1: Electron microprobe analyses of Na, K, and Fe in plagioclase; mg partitioning with orthopyroxene. *Proc. 10th Lunar Planet. Sci. Conf.* 627-638.
- Hodges C.A., Muelberger W.R. and Ulrich G.E. (1973) Geologic setting of Apollo 16. *Proc. 4th Lunar Sci. Conf.* 1-25.
- Hodges F.N. and Kushiro I. (1973) Petrology of Apollo 16 lunar highland rocks. *Proc. 4th Lunar Sci. Conf.* 1033-1048.
- Housley R.M., Cirlin E.H., Goldberg I.B. and Crowe H. (1976) Ferromagnetic resonance studies of lunar core stratigraphy. *Proc. 7th Lunar Sci. Conf.* 13-26.
- Hubbard N.J., Rhodes J.M., Gast P.W., Bansal B.M., Shih C.-Y., Wiesmann H. and Nyquist L.E. (1973b) Lunar rock types: The role of plagioclase in non-mare and highland rock types. *Proc. 4th Lunar Sci. Conf.* 1297-1312.
- Hubbard N.J., Rhodes J.M., Wiesmann H., Shih C.Y. and Bansal B.M. (1974) The chemical definition and interpretation of rock types from the non-mare regions of the Moon. *Proc. 5th Lunar Sci. Conf.* 1227-1246.
- Huneke J.C., Radicati di Brozolo F. and Wasserburg G.J. (1977) ⁴⁰Ar-³⁹Ar measurements on lunar highlands rocks with primitive ⁸⁷Sr/⁸⁶Sr (abs). *Lunar Sci. VIII*, 481-483. Lunar Planetary Institute, Houston.
- James O.B. (1981) Petrologic and age relations of the Apollo 16 rocks: Implications for subsurface geology and the age of the Nectaris Basin. *Proc. 12th Lunar Planet. Sci. Conf.* 209-233.
- Kerridge J.F., Kaplan I.R., Petrowski C. and Chang S. (1975) Light element geochemistry of Apollo 16 rocks and soils. *Geochim. Cosmochim. Acta* **39**, 137-162.
- Krahenbuhl U., Ganapathy R., Morgan J.W. and Anders E. (1973b) Volatile elements in Apollo 16 samples: Implications for highland volcanism and accretion history of the moon. *Proc. 4th Lunar Sci. Conf.* 1325-1348.
- Macdougall D., Rajan R.S., Hutcheon I.D. and Price P.B. (1973) Irradiation history and accretionary processes in lunar and meteoritic breccias. *Proc. 4th Lunar Sci. Conf.* 2319-2336.
- Mandeville J.-C. (1976) Microcraters on lunar rocks. *Proc. 7th Lunar Sci. Conf.* 1031-1038.

- Maurer P., Eberhardt P., Geiss J., Grogler N., Stettler A., Brown G.M., Peckett A. and Krahenbuhl U. (1978) Pre-Imbrium craters and basins: ages, compositions and excavation depths of Apollo 16 breccias. *Geochim. Cosmochim. Acta* **42**, 1687-1720.
- McGee P.E., Warner J.L., Simonds C.E. and Phinney W.C. (1979) Introduction to the Apollo collections. Part II: Lunar Breccias. Curator's Office. JSC
- Misra K.C. and Taylor L.A. (1975) Characteristics of metal particles in Apollo 16 rocks. *Proc. 6th Lunar Sci. Conf.* 615-639.
- Morris R.V., See T.H. and Horz F. (1986) Composition of the Cayley Formation at Apollo 16 as inferred from impact melt splashes. *Proc. 17th Lunar Planet. Sci. Conf.* in J. Geophys. Res. **90**, E21-E42.
- Nautiyal C.M., Padia J.T., Rao M.N. and Venkatesan T.R. (1981b) Solar flare neon: Clues from implanted noble gases in lunar soils and rocks. *Proc. 12th Lunar Sci. Conf.* 627-637.
- Nava D.F. (1974a) Chemical compositions of some soils and rock types from the Apollo 15, 16, and 17 lunar sites. *Proc. 5th Lunar Sci. Conf.* 1087-1096.
- Nyquist L.E., Hubbard N.J., Gast P.W., Bansal B.M., Wiesmann H. and Jahn B.M. (1973) Rb-Sr systematics for chemically defined Apollo 15 and 16 materials. *Proc. 4th Lunar Sci. Conf.* 1823-1846.
- Nyquist L.E. (1977) Lunar Rb-Sr chronology. *Phys. Chem. Earth* **10**, 103-142.
- Philpotts J.A., Schumann S., Kouns C.W., Lum-Staab R.K.L. and Schnetzler C.C. (1973b) Apollo 16 returned lunar samples – lithophile trace-element abundances. *Proc. 4th Lunar Sci. Conf.* 1427-1436.
- Rao M.N., Garrison D.H., Bogard D.D. and Reedy R.C. (1993) Solar-flare-implanted 4He/3He and solar-proton-produced Ne and Ar concentration profiles preserved in lunar rock 61016. *J. Geophys. Res.* **98**, 7827-7835.
- Rees C.E. and Thode H.G. (1974a) Sulfur concentrations and isotope ratios in Apollo 16 and 17 samples. *Proc. 5th Lunar Sci. Conf.* 1963-1973.
- Ryder G. and Norman M.D. (1979b) Catalog of pristine non-mare materials Part 2. Anorthosites. Revised. Curators Office JSC #14603
- Ryder G. and Norman M.D. (1980) Catalog of Apollo 16 rocks (3 vol.). Curator's Office pub. #52, JSC #16904
- See T.H., Horz F. and Morris R.V. (1986) Apollo 16 impact-melt splashes: Petrography and major-element composition. *Proc. 17th Lunar Planet. Sci. Conf.* in J. Geophys. Res. **91**, E3-E20.
- Smith J.V. and Steele I.M. (1974) Intergrowths in lunar and terrestrial anorthosites with implications for lunar differentiates. *Am. Mineral.* **59**, 673-680.
- Stettler A., Eberhardt Peter, Geiss J., Grogler N. and Maurer P. (1973) Ar39-Ar40 ages and Ar37-Ar38 exposure ages of lunar rocks. *Proc. 4th Lunar Sci. Conf.* 1865-1888.
- Stephenson A., Collinson D.W. and Runcorn S.K. (1974) Lunar magnetic field paleointensity determinations on Apollo 11, 16, and 17 rocks. *Proc. 5th Lunar Sci. Conf.* 2859-2871.
- Stöffler D., Schelien S. and Ostertag R. (1975) Rock 61016: Multiphase shock and crystallization history of a polymict troctolite-anorthosite breccia. *Proc. 6th Lunar Sci. Conf.* 673-692.
- Steele I.M. and Smith J.V. (1974) Mineralogy and petrology of some Apollo 16 rocks and fines: General petrologic model of the moon. *Proc. 4th Lunar Sci. Conf.* 519-536.
- Steele I.M., Hutcheon I.D. and Smith J.V. (1980) Ion microprobe analysis and petrogenetic interpretations of Li, Mg, Ti, K, Sr, Ba in lunar plagioclase. *Proc. 11th Lunar Planet. Sci. Conf.* 571-590.
- Tera F., Papanastassiou D.A. and Wasserburg G.J. (1973) A lunar cataclysm at 3.95 AE and the structure of the lunar crust (abs). *Lunar Sci. IV*, 723-725 Lunar Planetary Institute, Houston.
- Tera F., Papanastassiou D.A. and Wasserburg G.J. (1974a) Isotopic evidence for a terminal lunar cataclysm. *Earth Planet. Sci. Lett.* **22**, 1-21.
- Turner G. (1977a) Potassium-argon chronology of the moon. *Phys. Chem. Earth* **10**, 145-195.
- Turner G. (1977b) The early chronology of the Moon: Evidence for the early collisional history of the solar system. *Phil. Trans. Roy. Soc. London* **A285**, 97-104.
- Venkatesan T.R., Nautiyal C.M., Padia J.T. and Rao M.N. (1980) Solar flare cosmic ray proton fluxes in the recent past. *Proc. 11th Lunar Planet. Sci. Conf.* 1271-1284.
- Walker D., Longhi J., Grove T., Stolper E. and Hays J.F. (1973) Experimental petrology and origin of rocks from the Descartes Highlands. *Proc. 4th Lunar Sci. Conf.* 1013-1032.

Wrigley R.C. (1973) Radionuclides at Descartes in the central highlands. *Proc. 4th Lunar Sci. Conf.* 2203-2208.